EUROPHYSICS LETTERS 1 September 2003

Europhys. Lett., **63** (5), pp. 701–707 (2003)

Enhanced energy of parallel fractures in nacre-like composite materials

K. Okumura(*)

Physique de la Matière Condensée, Collège de France
11 place Marcelin Berthelot, 75231 Paris cedex 05, France and
Department of Physics, Graduate School of Humanities and Sciences
Ochanomizu University - 2-1-1, Otsuka, Bunkyo-ku, Tokyo 112-8610, Japan

(received 28 November 2002; accepted in final form 23 June 2003)

PACS. 46.50.+a – Fracture mechanics, fatigue and cracks.
PACS. 61.30.Dk – Continuum models and theories of liquid crystal structure.
PACS. 83.10.Ff – Continuum mechanics.

Abstract. – Nacre, often found inside sea shells such as oysters, has a spectacular resistance to fracture, which results from their construction out of alternating layers of soft and hard material. The fracture resistance is greatest for cracks moving perpendicular to the layers, but cracks parallel to the layers also have difficulty in progressing, and this fact has not been well explained. In this letter, we consider small parallel fractures in nacre-like material and show the possibility that the fracture energy is increased over a value due to the near-tip processes by a factor λ that is given by the ratio of short- and long-time viscoelastic moduli of the soft matter. Small cracks running along the layers take a scaling form we call a "lenticular trumpet" that has not previously been observed.

Introduction. – Nacre is a composite material with solid layers (aragonite) separated by thin slices of soft organic matter (proteins) (fig. 1). It has a spectacular toughness where a fracture propagates normal to the layers [1–4]. This toughness can be explained from the absence of stress concentration in this structure [5, 6]. In the present letter, we consider a different problem, where the fracture plane is parallel to the layers. The fracture properties have some similarity with those of a smectic liquid crystal, which have been discussed under the name of lenticular fracture where the bending effects of the layers are taken into account [7,8]. Our aim here is to consider the dynamics, when the soft layers behave like a viscoelastic fluid. But we shall start with a reminder of the statics: we summarize previous results obtained from the addition of the bending term in a simpler scaling argument.

The crucial feature is that, for a fracture cavity of size X along the layers, the elastically distorted zone has a size Y (perpendicular to the layers) which does not scale like X, but rather like

$$Y \simeq X^2/l \tag{1}$$

(*) E-mail: okumura@phys.ocha.ac.jp

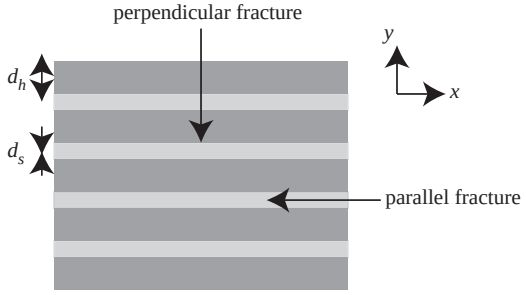

Fig. 1 – Nacre-type structure of materials: hard layers (elastic modulus E_h, thickness d_h) are glued together by soft layers (modulus E_s, thickness d_s). Cracks in the (y,z)-plane and the (x,z)-plane are called perpendicular and parallel fractures, respectively (the z-axis is perpendicular to this page).

for small cracks ($X \ll l$), where l is a characteristic length,

$$l^2 = K_\mathrm{B}/E_0. \tag{2}$$

Here K_B is the bending modulus and E_0 ($= E_\mathrm{s}d_\mathrm{h}/d_\mathrm{s}$) is an elastic modulus associated with the soft layers. In the following it is essential to note that *eq.* (1) *always holds at the scaling level*. (For larger cracks ($X > l$) the relation (1) turns back to $X \simeq Y$; this regime will be discussed elsewhere [9].)

For stratified materials, the following relation has been shown [8]:

$$l = d/\sqrt{\varepsilon}, \tag{3}$$

where

$$\varepsilon = \frac{E_\mathrm{s}}{E_\mathrm{h}} \cdot \frac{d_\mathrm{h}}{d_\mathrm{s}} \tag{4}$$

in the small-ε limit (see fig. 1 for notations). In the case of nacre, the small-crack condition $X \ll l$ is rather severe ($l \simeq 50d$). Thus, the following considerations might be more practical for some artificially synthesized layered composites where E_s (associated with the soft *weak gel*) is very small so that $l \gg d$.

The small-crack condition $X \ll l$ makes the situation different from the smectic liquid crystals: we have $Y \gg X$ because l corresponds to an atomic scale ($X/l \gg 1$ in eq. (1)) in the liquid-crystal case, [7] while, in the present case ($X/l \ll 1$), we have $X \gg Y$. *The anisotropic strain field is distributed widely in the x-direction compared to that in the y-direction* (see fig. 2 below) in our case.

The potential energy (per unit length in the z-direction) of the crack is dimensionally given as

$$F \simeq K_\mathrm{B}\left(\frac{u}{X^2}\right)^2 XY - \sigma u X + GX. \tag{5}$$

Here, u is the displacement in the y-direction, σ the pulling stress (along the y-axis) and G the fracture energy (energy required to create a new unit area). (It has been shown that the dominant component in strain and stress tensors are indeed the y components (u and σ, respectively) [8].) Note here that the first elastic term can be equally expressed as $E_0(u/Y)^2$ due to eq. (1); this term actually results from a local balance between these two elastic contributions and eq. (1) originates from this balance condition [7]. On minimizing F with respect

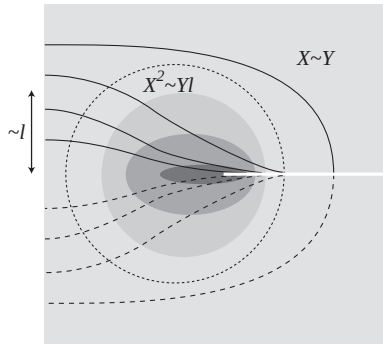

Fig. 2 – Scaling image of strain (stress) and deformation fields. Solid lines and broken lines are positive and negative deformation contours. Magnitudes of stress or strain are indicated by a gray scale (the darker the area, the larger the stress). The smaller the distance from the tip, the more anisotropic the behavior. Beyond a distance larger than l, the usual isotropic behavior is recovered. (Fracture studied in this paper is always limited to the case where $X \ll l$.)

to u, then, $F(X)$ has a maximum corresponding to the onset of fracture. At this critical state of fracture we have

$$u \sim X, \qquad \sigma \sim X^{-1}, \qquad \sigma u \simeq G, \tag{6}$$

where the last equation announces that *the product σu gives the fracture energy.* These fractures are very different from the conventional parabolic fractures in the linear elastic fracture mechanics [10] where the scaling laws are replaced with $u \sim X^{1/2}$ and $\sigma \sim X^{-1/2}$. In a more precise analysis, we have obtained forms for $u(x, y)$ and $\sigma(x, y)$, [8] which are consistent with eqs. (6) and (1).

Equation (1) states that, *at the scaling level, one point away from the tip by a distance X along the x-axis and another by a distance Y along the y-axis have the same order of strain (or stress), as long as $Y \simeq X^2/l$*; the situation can be *schematically represented* as in fig. 2.

We now proceed to the dynamics with employing a complex modulus of the form [7]

$$\mu(\omega) = E_0 + (E_\infty - E_0)\frac{i\omega\tau}{1 + i\omega\tau}\,, \tag{7}$$

where the ratio

$$\frac{E_\infty}{E_0} = \lambda$$

is assumed to be large as it is in a weakly cross-linked system. Here, E_0 is related to a small modulus associated with weak cross-links ($E_0 = E_\mathrm{s} d_\mathrm{h}/d_\mathrm{s}$), while E_∞ to a large modulus originating from entanglements. Equation (7) is a result of taking viscoelastic effects in soft layers through a complex modulus of the same form (but with E_0 and E_∞ replaced by E_s and λE_s) [9].

Crack shape and fracture energy. – We consider a parallel crack propagating with a constant speed V. When V is smaller than the sound velocity ($\simeq \sqrt{E_0/\rho}$), the equation of motion at the scaling level, $\rho Dv/Dt = -\nabla\sigma$ (with the density ρ and the local velocity v), reduces to a static equation: $\nabla\sigma = 0$. This is even true in our linear rheological model. In addition, the stress components must also satisfy a compatibility equations, which directly result from the definitions of strain fields (*i.e.* derivatives of deformation fields). But these geometric conditions, again, have the same scaling structures for our linear rheological model.

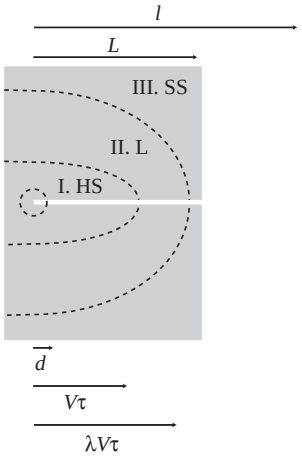

Fig. 3 – Three spatial regimes for our viscoelastic model. Due to the scaling relation $X^2 \simeq Yl$, the regions appear as anisotropic. The smallest region characterized by d has to be excluded from our arguments based on a continuum theory. Note that for a crack smaller than this figure with $V\tau < L < \lambda V\tau$ only the regions I and II are developed while for an even smaller crack with $d < L < V\tau$ only the region I is developed; this figure corresponds to a fully developed crack ($L > \lambda V\tau$). Note also that the degree of anisotropy of the boundaries separating regions are subject to the ratio of $V\tau$ or $\lambda V\tau$ to the length l; the smaller the ratio, the more anisotropic the behavior.

Thus, *the scaling relation for the stress in eq.* (6), $\sigma \sim 1/X \sim 1/\sqrt{Y}$, *remains unchanged even in our viscoelastic model*. These observations will be more precisely addressed elsewhere [9].

Another important observation here is the scaling identification of a distance X *along the* x*-axis* from the tip and the frequency ω via the speed V:

$$X \simeq V/\omega; \tag{8}$$

small distances correspond to high frequencies, while long distances to low frequencies —the farther away from the tip, the more time for relaxation. In addition, from eq. (1), the same magnitude of strain with the point specified by the above X is developed at a point separated from the tip by a distance Y ($\simeq X^2/l$) along the y-axis; these points have the same time ($1/\omega \simeq V/X$) to relax. Thus, a distance Y from the tip sees the same frequency ω but a slower propagating speed $V_y \simeq VX/l$ ($Y \simeq V_y/\omega$). In other words, we can imagine that fig. 2 correspond to a sequential propagation of the stress field (from the center outwards). We also note that, seen from a new coordinate $(x', y') = (x^2/l, y)$, the system returns to an isotropic system. For example, eqs. (6) are changed into the conventional parabolic form: $\sigma \sim 1/\sqrt{X'} \sim 1/\sqrt{Y'}$ and $u \sim \sqrt{X'} \sim \sqrt{Y'}$, etc.

Our viscoelastic model in eq. (7) has three regimes depending on frequencies: I, at high frequencies ($1 \ll \omega\tau$) it is like a solid with a large modulus $\mu(\omega) \simeq E_\infty$; II, at intermediate frequencies ($1/\lambda \ll \omega\tau \ll 1$) it is like a liquid with viscosity $\mu(\omega) \simeq i\omega\eta$, and III, at small frequencies ($\omega\tau \ll 1/\lambda$) it is like a soft solid with a small modulus $\mu(\omega) \simeq E_0$. Due to the correspondence between a distance and a frequency in eq. (8), a fracture can be thus spatially

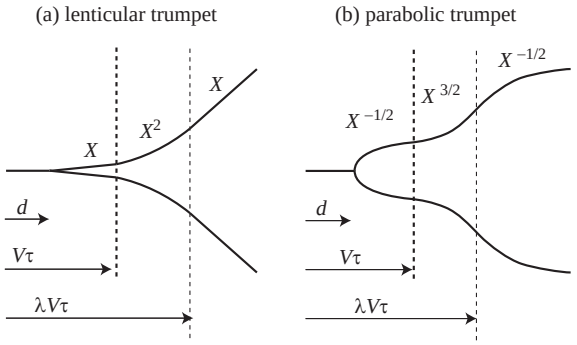

Fig. 4 – Lenticular and parabolic viscoelastic trumpets.

divided into three regions (fig. 3):

$$\begin{aligned} &\text{(I) } d \ll X \ll V\tau\text{:} && \text{hard solid (modulus } E_\infty\text{)},\\ &\text{(II) } V\tau \ll X \ll \lambda V\tau\text{:} && \text{liquid (viscosity } \eta\text{)},\\ &\text{(III) } \lambda V\tau \ll X\text{:} && \text{soft solid (modulus } E_0\text{)}. \end{aligned} \tag{9}$$

We consider a small-crack size L with $L \ll \lambda V\tau \ll l$ (larger-crack sizes ($L \gg l$) will be discussed elsewhere [9]); then, all the three regions I–III are fully developed. The soft-solid region III corresponds to low frequencies, and thus, to the static limit; in this region ($l \gg X \gg \lambda V\tau$), eqs. (6) hold. In the liquid zone (II), the stress field scales as $\sigma \simeq \omega\eta u/Y \simeq \eta V l u/X^3$ and at the same time it should scale as $\sigma \sim Y^{-1/2} \sim 1/X$ even in this liquid region as stated above. Thus, the strain should scale as $u \sim X^2$ and the product as $\sigma u \simeq X$. The coefficients can be determined by the matching at $X \simeq \lambda V\tau$ (the boundary between III and II):

$$\sigma u \simeq \frac{GX}{\lambda V\tau} \quad \text{(liquid zone)}. \tag{10}$$

In the hard-solid region of E_∞, we find $\sigma \simeq 1/\sqrt{Y}$ and $u \simeq \sqrt{Y}$ as in eqs. (6) but with $\sigma u \simeq G_0$ (via the same manner as in deriving eqs. (6)). Here, G_0 is associated with the hard solid appearing near the tip. Matching this latter product σu with that in eq. (10) at $X \simeq V\tau$, we find $G \sim \lambda G_0$. *The overall separation energy G for a fully developed crack is enhanced from G_0 associated with local processes near the tip.* Note here that this expression for G in our continuum theory is valid only for $d < V\tau$.

The crack shape resulting from this analysis is summarized as follows:

$$u \sim \begin{cases} X, & \text{for } \lambda V\tau < X,\\ X^2, & \text{for } V\tau < X < \lambda V\tau,\\ X, & \text{for } X < V\tau. \end{cases} \tag{11}$$

It is just like a trumpet with a lenticular edge (fig. 4a), as has been suggested by the name of the model, but different from previously known shapes; it is neither similar to the conventional parabolic form nor to an isotropic parabolic trumpet predicted [11] and observed [12] in certain polymer systems (fig. 4b).

We complete our arguments by considering smaller fractures. When $V\tau < L < \lambda V\tau$, only the hard-solid and liquid region are present; the soft solid has yet to develop. In this situation,

the fracture energy is given by eq. (10) at $X = L$, *i.e.* $G \simeq G_0 L/(V\tau)$; the toughness decreases with velocity. When $L < V\tau$, only the hard-solid region is developed and the fracture energy is given by G_0. Thus, with increase in V, the fracture energy starts from a larger plateau value λG_0, and then decreases to reach a smaller plateau value G_0:

$$G(V) \simeq \begin{cases} \lambda G_0, & \text{for } d/\tau < V < L/(\lambda\tau), \\ G_0 L/(V\tau), & \text{for } L/(\lambda\tau) < V < L/\tau, \\ G_0, & \text{for } L/\tau < V. \end{cases} \tag{12}$$

This behavior can be confirmed more precisely from a general formula:

$$\frac{G(V)}{G_0} \simeq E_\infty \int \frac{\mathrm{d}\omega}{\omega} \operatorname{Im}\left[\frac{1}{\mu(\omega)}\right], \tag{13}$$

which can be analytically calculated for the present model (just as in the previously known isotropic case [13]). It should be emphasized here that this formula is unaltered even in our anisotropic materials, which is by no means trivial; eq. (13) here can be shown in the following manner. We start from a relation:

$$G(V)V \simeq \int \mathrm{d}x \int \mathrm{d}y \sigma\dot{e} \simeq \int \mathrm{d}XY\sigma_X \dot{e}_X. \tag{14}$$

In order to estimate $\dot{e}_X$, we again use the dimensional identification in eq. (8): $\dot{e}_X \simeq \dot{e}_\omega \simeq \omega\sigma_\omega/\mu(\omega) \simeq \omega\sigma_X/\mu(\omega)$ and

$$G(V) \simeq \int \mathrm{d}\omega \frac{Y\sigma_X^2}{\omega\mu(\omega)} \simeq E_\infty G_0 \int \mathrm{d}\omega \frac{1}{\omega\mu(\omega)}\,. \tag{15}$$

Here, we have used a more precise form of eq. (6), $\sigma_X \simeq \sqrt{E_\infty G_0/Y}$, which should be valid for any frequency [9]. Since the real and imaginary parts of $1/\mu(\omega)$ are even and odd functions, respectively, we arrive at eq. (13).

Conclusion and discussion. – In this paper, we present a physical picture for fractures in nacre-type materials via scaling arguments. Viscoelastic effects for parallel fractures are taken into account via the simplest viscoelastic model for a weakly cross-linked polymer. We expect that for slow crack propagation speeds ($l \gg \lambda V\tau$) a small crack ($L \ll l$) takes a new trumpet shape different from previously reported shapes. The overall fracture energy G is enhanced from G_0 (associated with the hard-solid region originating from the entanglement effects) by a large factor λ for the fully developed cracks. With increase in velocity V, G is found to decrease from this large plateau value λG_0 to a smaller plateau value G_0.

Since G_0 is associated with the local process near the tip and in such a region there is no time for polymer molecules to perform the reptations, this energy might be comparable to that required to break chemical bonds and the value of G_0 experimentally observed in [12] (order of $\mathrm{J/m^2}$) is consistent with this interpretation.

The same line of study leads to the fracture energy of large cracks ($L \gg l$) enhanced by the same factor λ, although the crack shape is different. This case will be discussed elsewhere [9].

* * *

KO is grateful to P.-G. de Gennes for fruitful discussions and also for reading the drafts prior to submission with giving useful comments. KO also appreciates E. Raphaël and F. Saulnier for discussions. He thanks members of the group of PGG at Collège de France, including D. Quéré, for the warm hospitality during his third stay in Paris. This stay is financially supported by Collège de France.

REFERENCES

[1] Currey J. D., *Proc. R. Soc. London, Ser. B*, **196** (1977) 443.
[2] Jackson A. P., Vincent J. F. V. and Turner R. M., *Proc. R. Soc. London, Ser. B*, **234** (1988) 415.
[3] Song F. and Bai Y., *J. Mater. Res.*, **17** (2002) 1567.
[4] Evans A. G., Suo Z., Wan R. Z., Aksay I. A., He M. Y. and Hutchinson J. W., *J. Mater. Res.*, **16** (2001) 2475; Wang R. Z., Suo Z., Evans A. G., Yao N. and Aksay I. A., *J. Mater. Res.*, **16** (2001) 2485.
[5] de Gennes P.-G. and Okumura K., *C. R. Acad. Sci. Paris* t.1, Ser. IV (2000) 257.
[6] Okumura K. and de Gennes P.-G., *Eur. Phys. J. E*, **4** (2001) 121.
[7] de Gennes P. G., *Europhys. Lett.*, **13** (1990) 709.
[8] Okumura K., *Eur. Phys. J. E*, **7** (2002) 303.
[9] Okumura K., submitted to *Eur. Phys. J. E* (cond-mat/0212532).
[10] Anderson T. L., *Fracture Mechanics - Fundamentals and Applications* (CRC Press, Boca Raton) 1991.
[11] de Gennes P. G., *Langmuir*, **12** (1996) 4497.
[12] Ondarçuhu T., *J. Phys. II*, **7** (1997) 1893.
[13] Saulnier F., Raphaël E. and Ondarçuhu T., in preparation.